Rutgers, R., "Relative Viscosity of Suspensions of Rigid Spheres in Newtonian Liquids," *Rheol. Acta*, 2, 202-210 (1962).
Sweeney, K. H., and R. D. Geckler, "The Rheology of Suspensions," *J. Appl. Physics*, 25, 1135-1144 (1954).
Thomas, D. G., "Transport Characteristics of Suspension: VIII. A Note on the Viscosity of Newtonian Suspension of Uniform Spherical Particles," *J. Colloid Sci.*, 20, 267-277 (1965).

Manuscript received December 21, 1978; revision received October 16, and accepted November 6, 1978.

Effective Interfacial Area Determination by Gas Absorption Accompanied by Second-Order Irreversible Chemical Reaction

ERIK R. MATHERON
and
ORVILLE C. SANDALL
Department of Chemical and Nuclear Engineering
University of California
Santa Barbara, California

Oxygen and carbon dioxide were absorbed by aqueous sodium hydroxide solutions in an agitated vessel, and the experimental results were interpreted in terms of the surface renewal theory in order to deduce effective interfacial areas. The simultaneous physical and chemical absorption experiments permitted a determination of the enhancement factor under identical physicochemical and hydrodynamic conditions. It was found that for the unbroken interface case, the effective areas for physical and chemical absorption are equal when the Danckwerts parameter γ is approximately unity. γ is defined as the ratio of the increase in absorption capacity of the liquid to the enhancement factor. For the case where the gas is sparged through the liquid, it was found that the effective interfacial area is a strong function of agitator speed (above a critical speed) and gas flow rate, whereas the mass transfer coefficient was found to be nearly independent of agitator speed and gas sparge rate.

SCOPE

The interfacial area effective for mass transfer was measured for gas absorption in an agitated vessel. Experimental enhancement factors were determined for the irreversible second-order reaction between carbon dioxide and sodium hydroxide. Physical and chemical absorption rates were measured under identical physicochemical and hydrodynamic conditions by the simultaneous chemical absorption of carbon dioxide and the physical absorption or desorption of oxygen in aqueous solutions. The experimental enhancement factors together with theoretical solutions of the partial differential equations describing absorption accompanied by an irreversible second-order reaction according to the Higbie penetration or Danckwerts surface renewal theories allows an evaluation of the penetration time or surface renewal rate. The physical absorption mass transfer coefficient k_c° may then be predicted from a knowledge of the rate of surface renewal. Thus the effective interfacial areas may be determined from the measured values of the mass transfer coefficient times the effective interfacial area $k_c^\circ a$ and the predicted values of the mass transfer coefficient:

$$a = k_c^\circ a / k_c^\circ$$

Danckwerts and Joosten (1973) hypothesize that the effective area for chemical reaction depends on the type of reaction through the parameter γ, where γ is defined as the ratio of the factor by which the reaction increases the capacity of the liquid to absorb to the factor by which the reaction increases the rate of absorption:

$$\gamma = C/E$$

Experiments by Danckwerts and Joosten in a packed column show that when $\gamma \doteq 1$, the effective area for chemical absorption is equal to that for physical absorption and that when $\gamma >> 1$, the effective area is significantly greater for chemical absorption than for physical absorption. The reaction studied in this work, $CO_2 + 2OH^- \rightarrow CO_3^= + H_2O$, was chosen because it gives values of γ near unity. Previously used chemical absorption methods for determining effective interfacial areas have employed absorption accompanied by a rapid first-order chemical reaction with $\gamma >> 1$.

Experiments were carried out in an agitated vessel for the case of absorption across an unbroken interface and for the case where the gas is sparged through the liquid.

CONCLUSIONS AND SIGNIFICANCE

For the case of absorption across an unbroken interface, the penetration time was found to be sufficiently long so that it was not possible to operate outside of the instantaneous reaction regime for chemical absorption. As a result, the method could not be used to determine effective interfacial areas for absorption across an unbroken interface. However, in this case for $\gamma \doteq 1$, it was found that the effective area for physical absorption is equal to the effective area for chemical absorption. This was shown by comparing the experimentally determined physical absorption mass transfer capacity coefficient $k_c^\circ a$ with the physical absorption mass transfer capacity coefficient estimated from the chemical absorption experimental data and the theoretically predicted enhancement factor (Figure 2).

When the gas was sparged through the liquid, the penetration times were short enough so that the effective interfacial areas could be determined by the method proposed in this work. It was found in this case that the effective interfacial area is a strong function of agitation rate above a critical impeller speed of approximately 200 rev/min (Figure 5). It was also found that the effective area is very sensitive to the gas sparging rate (Figure 6). The mass transfer coefficient was found to be relatively insensitive to both the agitator speed and gas sparge rate (Figures 7 and 8).

It is usually not possible to directly measure the effective interfacial area a in gas absorption equipment; rather it is a combination of the mass transfer coefficient k_c° multiplied by the effective interfacial area which can be readily obtained from mass transfer rate measurements. However, since the process variables and pertinent physical properties may affect the mass transfer coefficient and the effective interfacial area in different ways, it is desirable to separate a from k_c° in order to obtain more meaningful correlations of these variables.

Chemical methods employing gas absorption accompanied by a fast first-order reaction have been developed to determine the effective interfacial area. Danckwerts and Joosten (1973) hypothesize that the effective area depends on the type of reaction through the parameter γ, where γ is defined as the ratio of the factor by which the reaction increases the capacity of the absorbant to the factor by which the reaction increases the rate of absorption. Experiments by Danckwerts and Joosten in a packed column show that when $\gamma \doteq 1$, the effective area is equal to that for physical absorption, and when $\gamma >> 1$, the effective area is significantly greater than for physical absorption.

In this research, the effective interfacial area for gas absorption in an agitated vessel was determined from simultaneous measurements of physical and chemical absorption rates. The experimental technique employed in this work, which was originally developed by Robinson and Wilke (1974), allows an evaluation of $k_c^\circ a$ and $k_c a$ under identical physicochemical and hydrodynamic conditions.

A second-order irreversible reaction was employed in our work, $CO_2 + 2OH^- \rightarrow CO_3^= + H_2O$, rather than the first-order reaction used by Robinson and Wilke and other previous workers. Use of a second-order reaction

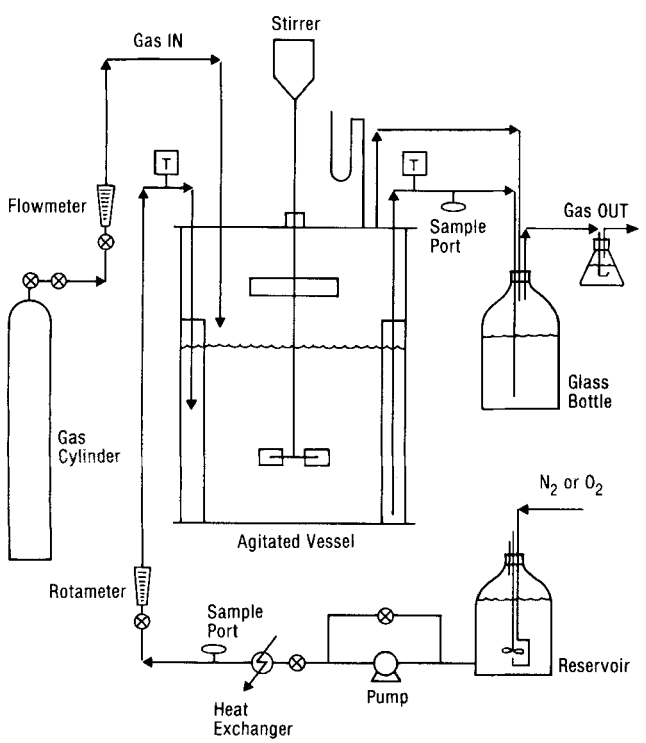

Fig. 1. Schematic drawing of gas absorption apparatus.

Table 1. Agitated Vessel Equipment Specifications

		Absorption column
[A]	Glass pipe	
	Length	304.8 mm
	Inside diameter	152.4 mm
[B]	Copper baffles	
	Length	203.2 mm
	Width	15.2 mm
	Thickness	1.6 mm
[C]	Liquid impeller	
	Stirring shaft diameter	12.7 mm
	Impeller diameter	50.8 mm
	Disk diameter	38.1 mm
	Height from tank bottom	50.8 mm
	Blade width	10.2 mm
	Blade length	12.7 mm
	Length of blade on disc	6.3 mm
[D]	Gas impeller	
	Stirring shaft diameter	12.7 mm
	Height from tank bottom	222.2 mm
	Impeller diameter	63.5 mm
	Blade width	7.6 mm
	Blade length	22.9 mm
[E]	Vessel tubes	
	Outside diameter	6.3 mm
	Inside diameter	4.0 mm
[F]	Gas sparging tube	
	Inside diameter	4.0 mm
	Height below impeller	31.7 mm

gives a γ value near unity, whereas first-order reactions usually give values of γ greater than ten.

The method used to determine the effective interfacial area is based on the Danckwerts surface renewal theory and was first suggested by Prasher (1975). The method may be explained as follows. The enhancement factor is determined experimentally from the simultaneous measurements of the physical and chemical absorption rates. Knowledge of the enhancement factor gives the surface renewal rate s from a solution of the differential equations describing the chemical absorption in terms of the surface renewal theory. Once the surface renewal rate is determined, the physical absorption mass transfer coefficient may be determined from

$$k_c^\circ = \sqrt{D_A s} \tag{1}$$

The effective interfacial area may then be determined from the measured rate of physical absorption:

$$a = \frac{(k_c^\circ a)}{k_c^\circ} \tag{2}$$

Thus, k_c° and a can be determined.

THEORY

The physical situation for the absorption of gas A followed by subsequent irreversible reaction with liquid phase reactant B ($A + 2B \rightarrow$ products) can be represented by a pair of time dependent diffusion equations:

$$\frac{\partial C_A}{\partial t} = D_A \frac{\partial^2 C_A}{\partial x^2} - kC_A C_B \tag{3}$$

$$\frac{\partial C_B}{\partial t} = D_B \frac{\partial^2 C_B}{\partial x^2} - 2kC_A C_B \tag{4}$$

The initial and boundary conditions are taken to be

$$\begin{aligned} &t = 0 \quad x > 0 \qquad C_B = C_{Bi} \quad C_A = 0 \\ &t > 0 \quad x = 0 \qquad \frac{\partial C_B}{\partial x} = 0 \qquad C_A = C_{Ao} \\ &t > 0 \quad x \rightarrow \infty \qquad C_B = C_{Bi} \quad C_A = 0 \end{aligned} \tag{5}$$

Equations (3) and (4) with boundary conditions given by Equation (5) have been solved numerically in dimensionless form using the Crank-Nicolson finite-difference procedure by Pearson (1963), Brian et al. (1961), and Matheron and Sandall (1978).

Matheron and Sandall used the results of their numerical calculation to deduce the enhancement factor for this reaction based on the Danckwerts surface renewal theory. It was found that the enhancement factors based on surface renewal theory differed only slightly from those based on the penetration theory. It was also found that the calculated enhancement factors were in excellent agreement with an approximate analytical equation derived by DeCoursey (1974)

$$E = \frac{-M}{2(E_a - 1)} + \left(\frac{M^2}{4(E_a - 1)} + \frac{E_a M}{(E_a - 1)} + 1 \right)^{1/2} \tag{6}$$

where E_a is the asymptotic value of the enhancement factor for an instantaneous reaction as given by Danckwerts (1970) and expressed by Equation (7):

$$E_a = 1/\text{erf}\, B \tag{7}$$

Where B is given by solution of the nonlinear Equation (8):

$$\frac{1}{2}\left(\frac{C_{Bi}}{C_{Ao}}\right)\left(\frac{D_B}{D_A}\right)^{1/2} \text{erf}\, B \exp B^2 = \text{erfc}\left[B\left(\frac{D_A}{D_B}\right)^{1/2} \right] \exp\left[\frac{B^2 D_A}{D_B} \right] \tag{8}$$

A comparison of the DeCoursey formula with the numerical results of Matheron and Sandall showed a maximum discrepancy in the enhancement factor of less than 7% over the range $0.2 \leq D_B/D_A \leq 5$ and for $0.2 \leq C_{Bi}/C_{Ao} \leq 10$. Thus, because of both the accuracy and simplicity of Equation (6), it was used to interpret the experimental results of this work.

EXPERIMENTAL APPARATUS AND PROCEDURE

Figure 1 is a schematic diagram of the mass transfer apparatus. The apparatus is similar to that used by Perez and Sandall (1974*a*). Table 1 lists the important geometrical characteristics of the mass transfer equipment. The absorption vessel was a 15.24 cm diameter glass pipe, 30.48 cm long, sealed on either end by an O ring and metal plate held down by a screwed clamp ring. The vessel was equipped with stirrers and four vertical baffles and was designed to conform to the standard tank configuration as described by Holland and Chapman (1964). Separate stirrers for the gas and liquid phases were mounted on a single shaft which went through a bearing in the top plate and was driven by a ¼ hp variable speed motor. The stirring shaft was sealed by an O ring and compressed teflon disk. The cross-sectional area of the gas-liquid interface was 179.5 cm^2. The liquid depth and liquid volume in the vessel were maintained, respectively, at 15.24 cm and 2.75 l. Four copper baffles 1.59 mm thick were soldered to the brass bottom plate at 90 deg intervals and extended vertically upward 20.32 cm and radially outward 1.52 cm from the vessel wall. The liquid agitator was a 5.08 cm diameter, six-blade disk mounted turbine impeller located 5.08 cm above the vessel bottom. The gas agitator was a 6.35 cm diameter six-blade open style turbine impeller located approximately in the middle of the gas phase. Stirrer speeds were determined using a stroboscope.

Unbroken Interface Experiments

The sodium hydroxide solution was prepared in a 50 l plastic reservoir. In order to obtain good accuracy for the measurement of the physical mass transfer coefficient, a low concentration of dissolved oxygen for the inlet solution was required. This requirement was met by bubbling nitrogen through the liquid for a few hours prior to starting the experiment. A stirrer was provided in order to homogenize the hydroxide concentrations and assist in the desorption of oxygen. The liquid phase left the reservoir through a tap placed at the bottom and was carried to the mass transfer vessel by a ⅛ hp self-priming pump. A heat exchanger was provided between the reservoir and the mass transfer vessel in order to maintain the liquid phase temperature in the tank at around 25°C. The flow rate was determined by a calibrated rotameter. A simple syphon placed between the agitated vessel and a 20 l glass bottle took care of the liquid circulation. The flow rate of the liquid leaving the glass bottle was controlled by a needle valve, and all the liquid phase was recovered in a plastic container in order to be recycled. Sample ports were provided both for the inlet and outlet liquid streams.

Oxygen (99.6% purity) and carbon dioxide (99.8% purity) were supplied from gas cylinders through pressure regulators. Gas flow rates were measured with calibrated rotameters and the gases were mixed before being saturated with water in a sparging bottle. In this case, the gas mixture entered and left the vessel above the liquid surface at a constant flow rate. After the gas left the mass transfer vessel, it flowed into the glass bottle containing the spent liquid. This procedure was followed in order to operate the vessel at about the same pressure as the mass transfer vessel so as to insure proper operation of the syphon. A liquid seal was then provided for the gas outlet by placing a 1 000 ml Erlenmayer flask in series with

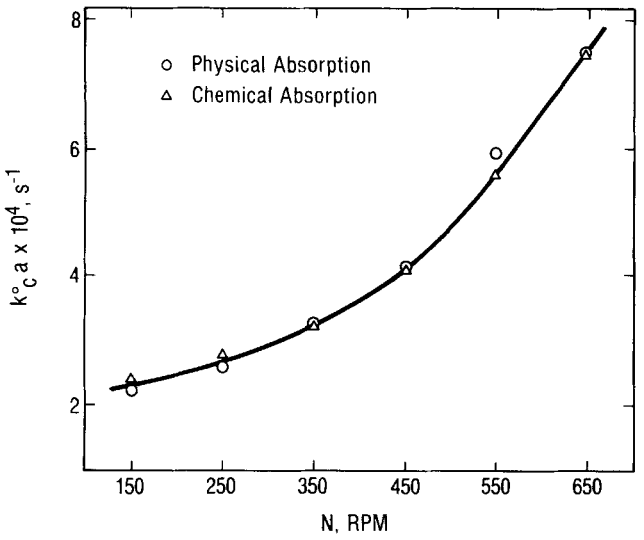

Fig. 2. Unbroken interface mass transfer capacity coefficients for physical adsorption determined by physical and chemical absorption as a function of impeller speed.

the glass bottle. A manometer measured the gas pressure above the mass transfer vessel.

Bubbling Experiments

Basically the same apparatus was used, but the solution was first saturated with oxygen instead of nitrogen. In these experiments, oxygen was desorbed from the solution. Desorption was preferred to absorption in this case because of the high efficiency of mass transfer when the gas was sparged through the liquid. Liquid phase outlet concentrations were found to be too close to saturation values for the case of absorption. However, in the case of desorption, it was possible to operate under conditions such that outlet liquid phase concentrations were significantly removed from saturation. Thus much better experimental accuracy for $k_c^\circ a$ was obtained by employing desorption rather than absorption.

In this case, a gas cylinder containing a gas mixture of carbon dioxide (approximately 20%) and nitrogen (approximately 80%) was used. A chromatographic analysis of this mixture was made in order to accurately determine its composition. The same flow system as in the first case was used, but the gas was introduced through a 4 mm ID sparge tube located in the liquid 3.17 cm directly below the turbine impeller.

Experimental Procedure

Liquid samples of approximately 25 ml were withdrawn by syringes from the inlet and outlet streams approximately 30 min after the agitation rate and gas flow rates were selected and the liquid heights in the tank and in the glass bottle had stabilized. A second set of samples was taken 15 min later as a check on the steady state operation. The concentrations relative to the chemical absorption were determined by a wet chemistry technique. A polarographic device was used to determine dissolved oxygen concentrations for the measurements relative to the physical absorption.

EXPERIMENTAL RESULTS AND DISCUSSION

Unbroken Interface

For this case, the surface renewal rates were found to be so low that the effective interfacial area could not be determined with sufficient accuracy. The enhancement factor is relatively insensitive to the surface renewal rate for low rates of renewal. Thus it was not possible to determine the effective area in this case. Data were taken, however, in the instantaneous reaction regime to verify that for $\gamma \doteq 1$, the effective area for chemical absorption is equal to the effective area for physical absorption.

To ensure that the data were obtained in the instantaneous reaction regime, the hydroxide concentrations were set so as to satisfy the Danckwerts (1970) criterion for an instantaneous reaction:

$$\frac{8D_A}{k_c^{\circ 2}} \frac{k}{s} C_{Bi} >> 4E_a^2 \tag{9}$$

The rate constant k was obtained from the literature as a function of temperature (Danckwerts and Sharma, 1966) and ionic strength (Nijsing et al., 1959).

Figure 2 shows the data obtained for the unbroken interface case plotted as the physical absorption mass transfer coefficient multiplied by the effective interfacial area vs. the impeller speed. $(k_c^\circ a)_{phys}$ was obtained by direct measurement, and $(k_c^\circ a)_{chem}$ was obtained by dividing $k_c a$ for chemical absorption by the predicted enhancement factor:

$$(k_c^\circ a)_{chem} = k_c a / E_a \tag{10}$$

As can be seen in Figure 2, $(k_c^\circ a)_{phys}$ shows good agreement with $(k_c^\circ a)_{chem}$, the maximum deviation being 6%. This indicates that for these experiments, the effective area for physical absorption is equal to the effective area for chemical absorption. γ in these experiments ranged from 0.85 to 0.96.

The mass transfer coefficients were calculated assuming perfect mixing in the liquid phase using Equations (11) and (12):

$$(k_c^\circ a)_{phys} = \frac{F}{V} \frac{(C_{O_2,2} - C_{O_2,1})}{(C_{O_2}^* - C_{O_2,2})} \left(\frac{D_{CO_2}}{D_{O_2}}\right)^{1/2} \tag{11}$$

$$k_c a = \frac{F}{V} \frac{(C_{OH^-,1} - C_{OH^-,2})}{2C_{CO_2}^*} \tag{12}$$

The square root of the ratio of the diffusivities of carbon dioxide and oxygen is included in Equation (11) in order to correct the mass transfer coefficient measured for oxygen to a value which would apply to carbon dioxide. The diffusivities of carbon dioxide and oxygen used in Equation (11) were taken to be those for pure water (Vivian and King, 1964) since the presence of ions is expected to affect D_{CO_2} and D_{O_2} in a similar way, and thus the ratio D_{CO_2}/D_{O_2} should not be affected. The saturation solubilities of oxygen, $C_{O_2}^*$, were measured using the polarographic device; the carbon dioxide solubilities were calculated from solubility data in the literature (Perez and Sandall, 1974*b*) and were corrected for the presence of ions in solution using the method of Nijsing and Kramers as given by Astarita (1967).

It is assumed in our analysis that the gas phase mass transfer resistance is negligible compared to the liquid phase resistance. This assumption was checked by estimating a maximum effect in the following way. A lower bound for the gas phase mass transfer coefficient was calculated assuming that the gas bubbles were rigid spheres with no circulation. An upper bound of 3% for the gas phase resistance was then estimated when the gas phase resistance so determined was compared to the minimum resistance found experimentally for the liquid phase.

Bubbling Case

For the case where the gas was sparged through the liquid, the surface renewal rate was so fast that the instantaneous reaction regime could not be achieved. Thus, in this case, plots such as Figure 2, showing that the effective areas for physical and chemical absorption are equal, could not be made. However, since the enhancement factor is quite sensitive to the surface renewal

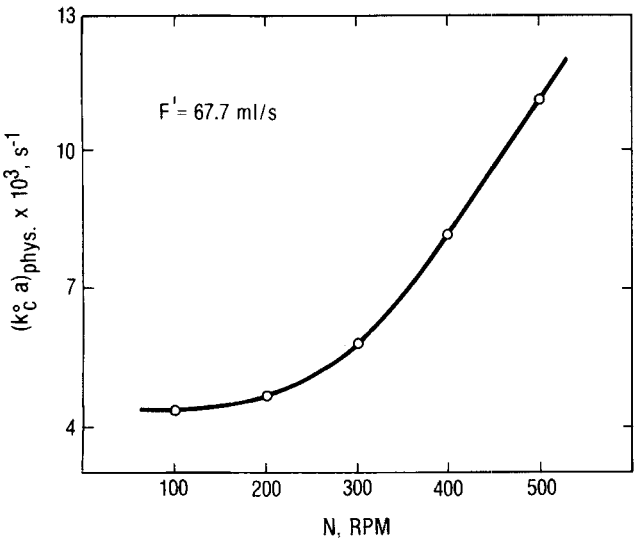

Fig. 3. Mass transfer capacity coefficient as a function of impeller speed $F = 67.7$ ml/s.

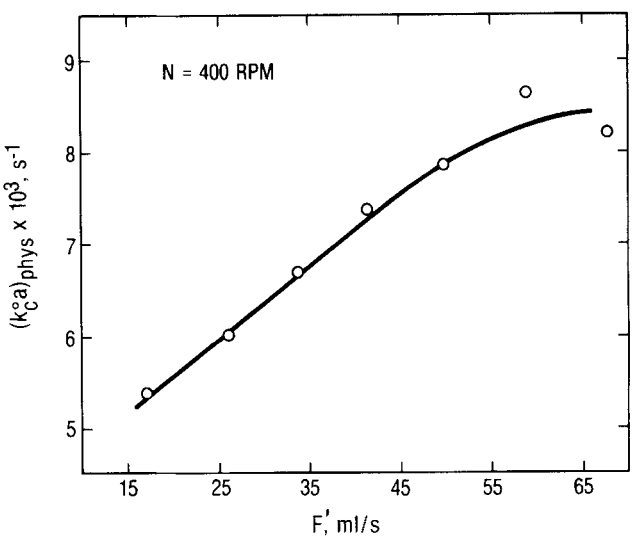

Fig. 4. Mass transfer capacity coefficient as a function of gas sparging rate. $N = 400$ rev/min.

rate for these fast renewal rates, the effective interfacial areas could be determined.

Mass transfer rates were large enough so that the partial pressures of oxygen and carbon dioxide changed significantly from the gas inlet to gas outlet condition. In order to determine the saturation or interfacial values of the liquid phase gas concentrations $C_{O_2}^*$ and $C_{CO_2}^*$, the arithmetic average partial pressures were used. It was thus assumed that the gas bubbles did not coalesce within the liquid phase, and hence there was no mixing within the dispersed gas phase.

Figure 3 shows the physical absorption mass transfer data plotted as a function of impeller speed for a constant gas sparge rate of 67.7 ml/s. It may be seen that the agitation speed has little effect on the mass transfer rate below impeller speeds of 200 rev/min.

Figure 4 shows the physical absorption mass transfer data plotted as a function of the gas sparging rate for a constant impeller speed of 400 rev/min. The mass transfer rate shows an almost linear relationship with gas flow rate. Table 2 summarizes the bubbling case experimental mass transfer data.

The effective interfacial areas as determined from the data in Table 2 are shown in Figures 5 and 6. Figure 5 shows that for a constant gas sparging rate of 67.7 ml/s, the interfacial area increases with increasing agitator speed. The effect of gas sparging rate on the interfacial area is shown in Figure 6. For a constant impeller speed of 400 rev/min, the data in Figure 6 show that the effective interfacial area is quite sensitive to the gas sparging rate.

Figures 7 and 8 show the mass transfer coefficients for physical absorption as determined by the calculated surface renewal rates. Calderbank (1958) has considered power requirements for agitation in sparged vessels for an impeller geometry identical to ours. Using his correlation, we can show that for the conditions of our experiments, power input increases with impeller speed for a constant gas sparge rate. In Figure 7 it is seen that the

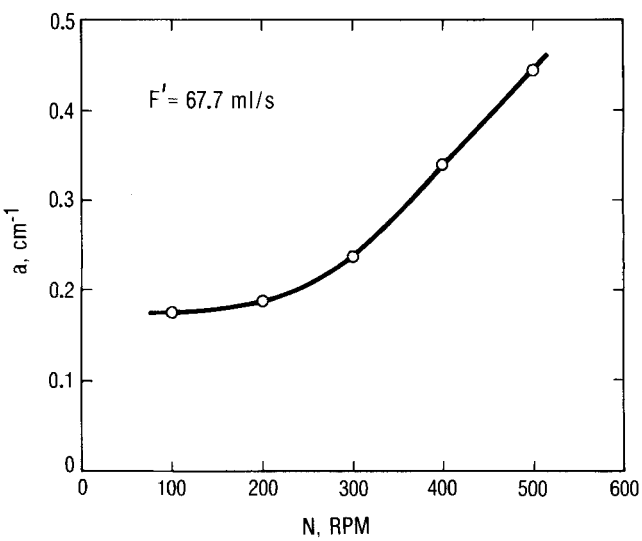

Fig. 5. Effective interfacial area per unit volume as a function of impeller speed. $F = 67.7$ ml/s.

Table 2. Bubbling Case Mass Transfer Data

Run	T (°C)	N (rev/min)	F', ml/s	$\frac{C_{OH^-}}{C^*_{CO_2}}$	E(exp.)	$(k^\circ_c a)_{phys.} \times 1\,000\ (s^{-1})$	$k_c^\circ \times 100$ (cm/s)	a(cm²)	γ
1	27.1	100	67.7	12.9	3.65	4.37	2.45	490	2.0
2	24.6	200	67.7	15.8	3.80	4.67	2.47	520	2.4
3	25.7	300	67.7	10.5	3.14	5.84	2.44	658	2.0
4	24.6	400	67.7	10.1	2.96	8.22	2.42	934	2.0
5	25.8	500	67.7	5.3	2.18	11.13	2.50	1 224	1.7
6	24.9	400	17.0	18.4	2.66	5.36	3.66	403	3.9
7	24.6	400	26.0	11.7	2.63	5.99	2.82	584	2.6
8	24.6	400	33.7	7.5	2.35	6.68	2.76	666	2.0
9	24.6	400	41.3	9.8	2.64	7.37	2.73	742	2.2
10	24.6	400	49.8	7.7	2.52	7.84	2.53	852	1.9
11	24.6	400	58.8	6.1	2.31	8.66	2.50	951	1.7

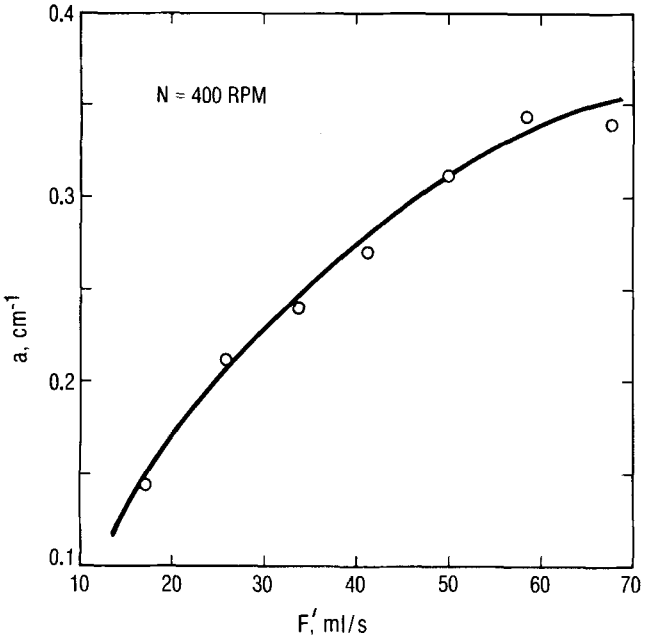

Fig. 6. Effective interfacial area per unit volume as a function of gas sparging flow rate.

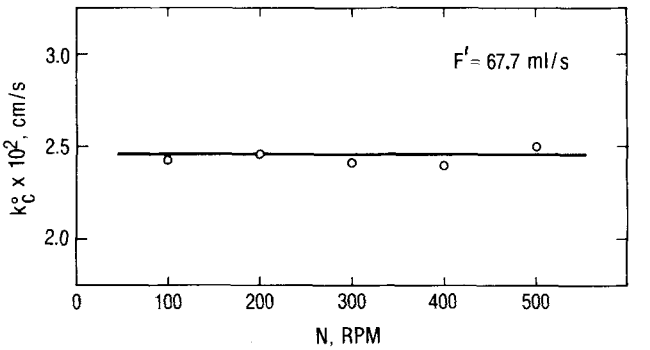

Fig. 7. Mass transfer coefficient as a function of impeller speed. Gas sparging flow rate = 67.7 ml/s.

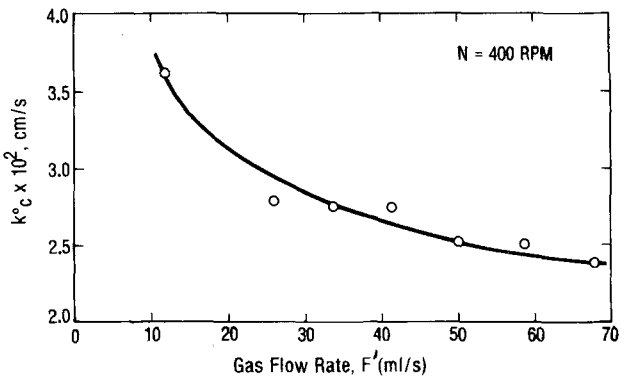

Fig. 8. Mass transfer coefficient as a function of gas sparging flow rate. Impeller speed = 400 rev/min.

mass transfer coefficient is independent of impeller speed, thus, increasing the impeller speed or the power input to the agitated vessel increases the interfacial area but has no effect on the mass transfer coefficient. The effect of increasing the gas sparging rate on the mass transfer coefficient for a constant impeller speed of 400 rev/min in shown in Figure 8. The power requirement results of Calderbank (1958) indicate that for a constant agitation rate, the power input decreases with increasing gas flow rate. For gas flow rates greater than 25 ml/s, the mass transfer coefficient is relatively insensitive to the gas flow rate. A possible explanation for the decrease in $k_c°$ with increasing gas flow rate at the lower gas sparge rates is that at the lowest flow rate the gas bubbles remain in the central region of the agitated vessel where the surface renewal rate is high. As the gas flow rate increases, the gas bubbles become more uniformly distributed throughout the vessel, and therefore the average surface renewal rate becomes lower.

For these experiments, γ ranged from 1.7 to 2.6 except for one run for $\gamma = 3.9$. This range in γ was about as low as could be achieved experimentally in order to have good accuracy in the determination of the surface renewal rate. Thus, γ for these experiments was not as close to unity as for the unbroken interface experiments in which it was shown that the effective interfacial area for chemical absorption is equal to that for physical absorption under identical physicochemical and hydrodynamic conditions. However, the values of γ for these bubbling experiments were at least an order of magnitude lower than for previous experimental effective area determinations employing first-order kinetics. Thus, the hypothesis that $a_{\text{chem}} = a_{\text{phys}}$ should be more closely satisfied for our experiments.

NOTATION

a = effective interfacial area per unit volume, cm^{-1}
C_A = concentration of dissolved gas, g mole/cm^3
C_{Ao} = interfacial concentration of dissolved gas, g mole/cm^3
C_B = concentration of liquid phase reactant, g mole/cm^3
C_{Bi} = concentration of liquid phase reactant in the bulk liquid, g mole/cm^3
$C_{CO_2}^*$ = interfacial concentration of carbon dioxide, g mole/cm^3
$C_{O_2,1}$ = inlet concentration of oxygen, g mole/cm^3
$C_{O_2,2}$ = outlet concentration of oxygen, g mole/cm^3
$C_{O_2}^*$ = interfacial concentration of oxygen, g mole/cm^3
$C_{OH^-,1}$ = inlet concentration of oxygen, g mole/cm^3
$C_{OH^-,2}$ = outlet concentration of hydroxide, g mole/cm^3
D_A = diffusivity of dissolved gas, cm^2/s
D_B = diffusivity of liquid phase reactant, cm^2/s
D_{CO_2} = diffusivity of carbon dioxide, cm^2/s
D_{O_2} = diffusivity of oxygen, cm^2/s
E = enhancement factor $\equiv k_c/k_c°$
E_a = asymptotic value of the enhancement factor given by Equation (7)
F = volumetric liquid flow rate, cm^3/s
F' = volumetric gas flow rate, cm^3/s
k = second-order reaction rate constant, cm^3/g mole s
k_c = mass transfer coefficient for chemical absorption, cm/s
$k_c°$ = mass transfer coefficient for physical absorption, cm/s
$(k_c°)_{\text{phys}}$ = physical absorption mass transfer coefficient determined from physical absorption experiments, cm/s
$(k_c°)_{\text{chem}}$ = physical absorption mass transfer coefficient determined from chemical absorption experiments, cm/s
M = $D_A k C_{Bi}/(k_c°)^2$
s = rate of surface renewal, s^{-1}
V = volume of liquid in agitated vessel, cm^3
x = distance measured into the liquid from the free surface, cm
γ = ratio of the increase in capacity of the solution to absorb a gas to the enhancement factor
τ = penetration time, s

LITERATURE CITED

Astarita, G., *Mass Transfer with Chemical Reaction*, Elsevier, New York (1967).

Brian, P. L. T., J. F. Hurley, and E. H. Haseltine, "Penetration Theory for Gas Absorption Accompanied by a Second Order Chemical Reaction," *AIChE J.*, 7, 226 (1961).

Calderbank, P. H., "Physical Rate Processes in Industrial Fermentation, Part 1: The Interfacial Area in Gas-Liquid Contacting with Mechanical Agitation," *Trans. Inst. Chem. Engrs.*, 36, 443 (1958).

Danckwerts, P. V., *Gas-Liquid Reactions*, p. 39, McGraw-Hill, New York (1970).

———, and G. E. H. Joosten, "Chemical Reaction and Effective Interfacial Areas in Gas Absorption," *Chem. Eng. Sci.*, 28, 453 (1973).

Danckwerts, P. V., and M. M. Sharma, "The Absorption of Carbon Dioxide into Solutions of Alkali and Amines," *Chem. Engr.*, 44, CE 244 (1966).

DeCoursey, W. J., "Absorption with Chemical Reaction: Development of a New Relation for the Danckwerts Model," *Chem. Eng. Sci.*, 29, 1867 (1974).

Holland, F. A., and F. S. Chapman, *Liquid Mixing and Processing in Stirred Tanks*, p. 11, Reinhold, New York (1964).

Matheron, E. R., and O. C. Sandall, "Gas Absorption Accompanied by a Second Order Chemical Reaction Modeled According to the Danckwerts Surface Renewal Theory," *AIChE J.*, 24, 552 (1978).

Nijsing, R. A. O. T., R. H. Hendrikez, and H. Kramers, "Absorption of CO_2 in Jets and Falling Films of Electrolyte Solutions, With and Without Chemical Reaction," *Chem. Eng. Sci.*, 10, 88 (1959).

Pearson, J. R. A., "Diffusion of One Substance into a Semi-Infinite Medium Containing Another with Second-Order Reaction," *Appl. Sci. Res.*, A11, 321 (1963).

Perez, J. F., and O. C. Sandall, "Gas Absorption by Non-Newtonian Fluids in Agitated Vessels," *AIChE J.*, 20, 770 (1974*a*).

———, "Carbon Dioxide Solubility in Aqueous Carbopol Solutions at 24°, 30° and 35°C," *J. Chem. Eng. Data*, 19, 51 (1974*b*).

Prasher, B. D., "Mass Transfer Coefficients and Interfacial Areas in Agitated Dispersions," *AIChE J.*, 21, 407 (1975).

Robinson, C. W., and C. R. Wilke, "Simultaneous Measurement of Interfacial Area and Mass Transfer Coefficients for a Well-Mixed Gas Dispersion in Aqueous Electrolyte Solutions," *ibid.*, 20, 285 (1974).

Vivian, J. E., and C. J. King, "Diffusivities of Slightly Soluble Gases in Water," *ibid.*, 10, 220 (1964).

Manuscript received January 13, 1978; revision received September 29, and accepted October 5, 1978.

The Co-current Reactor Heat Exchanger:

Part I. Theory

THOMAS F. DEGNAN

and

JAMES WEI

Chemical Engineering Department
University of Delaware
Newark, Delaware 19711

Mathematical development is presented for the theory of a reactor heat exchanger in which the heat generated in the reaction stream is simultaneously transferred to a co-currently flowing coolant stream. The advantages of this scheme include isothermal conditions for the reaction stream, decreased parametric sensitivity, and improved stability.

SCOPE

Catalytic reactions which liberate (or absorb) large quantities of heat must have specially designed reactors to deal with them. Temperature excursions caused by insufficient cooling can lead to premature aging of the catalysts, production of undesirable side products, a shift of thermodynamic equilibrium against the completion of the reaction, or ultimately to the destruction of the reaction vessel. It is necessary to control the temperature deviations and to manage the temperature profile for the maximum yield of product. Numerous schemes have been employed (Froment, 1974).

This paper describes a theoretical analysis of a reactor heat exchanger that combines many of the desirable traits of current designs. Attainment of isothermal condition for reactant stream, parametric sensitivity, and stability of autothermal systems are considered.

CONCLUSIONS AND SIGNIFICANCE

The theory of a co-current reactor heat exchanger is presented and has led to the design of a reactor where the reaction stream remains isothermal in spite of highly exothermal reactions. It is shown that the isothermal design is easiest to obtain for first-order rate expressions and is extended to reactions of arbitrary order and to Langmuir-Hinshelwood kinetics. In each of these nonfirst-order cases, nonuniform catalyst distribution in the direction of flow is required.

An isothermal reactant stream is attained only at narrow windows of design and operation variables. These windows are defined by an exact balance between heat generation by exothermic reaction and heat removal by transport to the coolant stream. Outside of the window, the reactant stream either heats up or cools down.

Thomas F. Degnan is with the Minnesota Mining and Manufacturing Company, 3M Center, Saint Paul, Minnesota 55101. James Wei is with the Department of Chemical Engineering, Massachusetts Institute of Technology, Cambridge, Massachusetts 02139.